Stem Cell Research & Therapy

RESEARCH

Open Access

Activation of angiopoietin-1 signaling with engineering mesenchymal stem cells promoted efficient angiogenesis in diabetic wound healing

Qiong Deng[1†], Fangzhou Du[1†], Shenzhen Pan[1,4], Yuchen Xia[1,2], Yuxin Zhu[1,2], Jingzhong Zhang[1,2,3*], Chenglong Li[4*] and Shuang Yu[1,2,3*]

Abstract

Background Vascular insufficiency is associated with the pathogenesis and therapeutic outcomes of diabetic foot ulcers (DFU). While mesenchymal stem cells (MSCs) hold potential for DFU treatment, further enhancement in promoting angiogenesis in the challenging DFU wounds is imperative.

Methods The differential expression of pro- and anti-angiogenic factors during both normal and diabetic wound healing was compared using quantitative PCR. MSCs derived from the umbilical cord was prepared, and the engineered MSC (MSC^{ANG1}) overexpressing both the candidate pro-angiogenic gene, angiopoietin-1 (ANG1), and green fluorescent protein (GFP) was constructed using a lentiviral system. The pro-vascular stabilizing effects of MSC^{ANG1} were assessed in primary endothelial cell cultures. Subsequently, MSC^{ANG1} was transplanted into streptozotocin (STZ)-induced diabetic wound models to evaluate therapeutic effects on angiogenesis and wound healing. The underlying mechanisms were further examined both in vitro and in vivo.

Results The comprehensive analysis of the temporal expression of pro- and anti-angiogenic factors revealed a consistent impairment in ANG1 expression throughout diabetic wound healing. MSC^{ANG1} exhibited robust EGFP expression in 80% of cells, with overexpression and secretion of the ANG1 protein. MSC^{ANG1} notably enhanced the survival and tubulogenesis of endothelial cells and promoted the expression of junction proteins, facilitating the establishment of functional vasculature with improved vascular leakage. Although MSC^{ANG1} did not enhance the survival of engrafted MSCs in diabetic wounds, it significantly promoted angiogenesis in diabetic wound healing, fostering the establishment of stable vasculature during the healing process. Activation of the protein kinase B (Akt)

[†]Qiong Deng and Fangzhou Du contributed equally to this work.

*Correspondence:
Jingzhong Zhang
zhangjz@sibet.ac.cn
Chenglong Li
chenglongli2012@suda.edu.cn
Shuang Yu
yush@sibet.ac.cn

Full list of author information is available at the end of the article

© The Author(s) 2025. **Open Access** This article is licensed under a Creative Commons Attribution-NonCommercial-NoDerivatives 4.0 International License, which permits any non-commercial use, sharing, distribution and reproduction in any medium or format, as long as you give appropriate credit to the original author(s) and the source, provide a link to the Creative Commons licence, and indicate if you modified the licensed material. You do not have permission under this licence to share adapted material derived from this article or parts of it. The images or other third party material in this article are included in the article's Creative Commons licence, unless indicated otherwise in a credit line to the material. If material is not included in the article's Creative Commons licence and your intended use is not permitted by statutory regulation or exceeds the permitted use, you will need to obtain permission directly from the copyright holder. To view a copy of this licence, visit http://creativecommons.org/licenses/by-nc-nd/4.0/.

pathway and suppression of proto-oncogene tyrosine kinase Src (Src) activity in MSC^{ANG1}-treated diabetic wounds confirmed efficient angiogenesis process. Consequently, epidermal and dermal reconstruction, as well as skin appendage regeneration were markedly accelerated in MSC^{ANG1}-treated diabetic wounds compared to MSC-treated wounds.

Conclusion Treatment with MSCs alone promotes angiogenesis and DFU healing, while the engineering of MSCs with ANG1 provides substantial additional benefits to this therapeutic process. The engineering of MSCs with ANG1 presents a promising avenue for developing innovative strategies in managing DFU.

Keywords Mesenchymal stem cells, Angiopoietin-1, Diabetic Wound Healing, Angiogenesis, Vascular leakage

Introduction

The global population of individuals with type 2 diabetes (T2D) is increasing, currently exceeding 500 million [1]. It is reported that around 20% of these patients will suffer from non-healing diabetic foot ulcers (DFU). Due to the absence of a definitive healing protocol, DFU can progress to necrosis or even necessitate amputation, causing significant distress to patients and imposing a heavy burden on society [2].

Vascular insufficiency is closely associated with the onset and prognosis of DFU [3]. The restoration of functional vascularity is crucial among the various treatment approaches for DFU. Despite significant progress in enhancing angiogenesis in diabetic wounds through the supplementation of angiogenic cells or growth factors, challenges with degradation and uncontrolled release, safety issues, and economic burdens have limited the clinical translation of these advancements [4, 5]. Mesenchymal stem cells (MSCs), renowned for their immunoregulatory and pro-regenerative capabilities, hold substantial promise in treating a range of critical diseases. While MSCs-based therapies have shown safety and effectiveness in addressing DFU, their efficacy is compromised by the unfavorable pathological conditions in DFU. One promising strategy to enhance the therapeutic efficacy of MSCs therapy in DFU involves genetically modifying MSCs to incorporate specific therapeutic molecules, such as appropriate angiogenic factors, customized to the specific pathological conditions of DFU.

Angiopoietin-1 (ANG1), a 70 kDa glycoprotein belonging to the angiopoietin family, is synthesized by perivascular support cells such as pericytes and vascular smooth muscle cells [6, 7]. It exerts its effects by binding specifically to the Angiopoietin-Tie receptor 2 (Tie2) receptor through a paracrine mechanism, which leads to the phosphorylation of the Tie2 receptor on endothelial cells and facilitates the maturation and stabilization of new blood vessels [6, 7]. In the context of wound healing, ANG1 plays a critical role in the angiogenic process by promoting endothelial cell survival and migration, as well as the recruitment and maturation of pericytes. Notably, ANG1 plays a significant role for enhancing vascular maturation and stability and preventing leakage [6]. However, MSCs generally do not produce adequate levels of ANG1. Previous studies have demonstrated that bone marrow-derived MSCs engineered with the ANG1 gene could significantly enhance wound healing in normal wound models by providing a sufficient supply of ANG1 [8]. However, the expression levels of pro- and anti-angiogenic factors underlying the impaired DFU angiogenesis, as well as the therapeutic effects of ANG1-engineered MSCs on the ischemic DFU, are still not fully understood.

In the present study, we conducted a comparative analysis of the dynamic changes in angiogenic factors during normal and diabetic wound healing. Our findings revealed a significant impairment of ANG1 throughout the process of diabetic wound healing when compared to normal healing. To address this, we constructed trackable engineered MSCs (MSC^{ANG1}) stably expressing angiogenic factor ANG1 and green fluorescent protein (GFP). Although the overexpression of ANG1 did not directly improve the survival of transplanted MSCs, it significantly enhanced angiogenesis and promoted diabetic wound healing. Moreover, MSC^{ANG1} demonstrated a notable influence on the survival, migration, and formation of functional tight junctions in endothelial cells through activation of Akt/mTOR pathway and inhibition of Src pathway,

Methods

Preparation of the primary MSCs and endothelial culture

All studies involved with human samples were performed in accordance with the 'Ethical Guiding Principles on Human Embryonic Stem Cell Research' and Helsinki Declaration. Umbilical cords were donated with the signed informed consent and ethical approval from the first affiliated hospital of Soochow University (2019 – 136). MSCs were isolated and cultured as previously described [9, 10]. Briefly, Wharton's jelly in the umbilical cord was dissected and minced into 1-mm^3 pieces, followed by inoculation in Dulbecco's modified Eagle's medium (DMEM)/F12 medium (D/F; BC–M–002, Bio-Channel, China) with 10% fetal bovine serum (FBS; FND500, ExCell, China). The tissue blocks were removed when cells reached 50% confluence.

Human umbilical vein endothelial cells (HUVECs) were isolated as previously described [11]. Briefly, collagenase was injected into the umbilical vein, and the digest was subsequently collected and centrifuged to obtain cells. Cells were plated and maintained in an endothelial culture medium (ECM; 1001, Sciencell, USA) [12].

Lentivirus production and preparation of engineered MSCs

The coding sequence (CDS) fragment of mouse ANG1 (NM_009640.4) was synthesized (Miaoling, China), and incorporated into the lentiviral plasmid pLVX-CMV-EGFP (Miaoling, China) through t2A linker to prepare pLVX-CMV-ANG1-EGFP plasmid.

The lentivirus ANG1-EGFP or EGFP were generated in HEK 293T cells co-transfected with three package plasmids and pLVX-CMV-ANG1-EGFP or pLVX-CMV-EGFP lentiviral vectors, respectively [9]. The MSCs were infected with lentivirus at MOI = 1 in the D/F medium supplemented with 8 μg/mL of polybrene (40804ES, Yeasen, China) for 5–6 h. 48 h later, GFP immunostaining was used to determine the purity of engineered MSCs, and the culture with > 70% MSCs expressed GFP was used for the subsequent experiments.

Cell treatment

For preparation of the conditional medium (CM), MSC^{GFP} or MSC^{ANG1} (P3-P5) were washed, and re-fed with serum-free D/F medium. 48 h later, the medium was collected and centrifuged at 2000 g for 5 min. The supernatant was then harvested and stored at -80 ℃. The D/F medium incubated without MSCs for 48 h was set as control (Ctrl).

The primary HUVECs plated at a density of 5×10^5/well in 6-well plates and cultured until they reach 70–80% confluence. Cells were washed with PBS, followed by incubation with D/F containing 50% of CM or Ctrl for 48 h. HUVECs cultured with D/F containing 200 ng/mL ANG1 (HY-P74412A, MCE, USA) were set as positive controls.

Evaluation of cell viability

The cell viability was evaluated using an Annexin V-FITC/PI apoptosis detection kit (V13241, Invitrogen, USA) or Calcein-AM/PI double stain kit (C2015S, Beyotime, China). For Annexin V-FITC/PI staining, HUVECs were detached using 0.25% trypsin, followed by incubation with 5 μL of Annexin V-FITC and 5 μL of Propidium Iodide (PI) at RT for 30 min. Stained cells were analyzed using a Novo Cyte 2000R (Agilent, USA), and data were analyzed using NovoExpress software version 1.5.0 (Agilent, USA). For Calcein-AM and PI staining, HUVECs were incubated with Calcein-AM and PI for 30 min at 37 °C. The images were acquired using a fluorescent microscope (×100 magnification; NIB900, NOVEL, China) and analyzed with ImageJ software (National Institutes of Health, USA).

Tube formation assay

In vitro angiogenesis assays were performed using Matrigel basement membrane matrix (354277, Corning, USA) according to the manufacturer's instructions. Matrigel was thawed overnight at 4 °C and added to pre-chilled 96-well plates and incubated to solidify at 37 °C for 30 min. HUVECs were plated, treated with ECM containing 50% of CM or Ctrl for 4 h as described previously [13, 14]. The tube formation images were acquired using a phase-contrast microscope (×100 magnification; NIB410, NOVEL, China). The experiment was replicated three times and the total length of tubes in five randomly selected regions per well was measured using ImageJ software.

In vitro permeability assay

HUVECs were grown onto transwell membrane with 0.4 μm pore size (353095, Falcon, China) till confluent, and incubated with ECM containing 50% of CM or Ctrl for 48 h. The tracer FITC-labeled dextran (1 mg/mL) was added to the top chamber for 45 min. Then the intensity of FITC in the bottom chamber was measured at a wavelength of 520 nm (Excitation: 485 nm) with a microplate reader (Varioskan LUX, Thermo, USA).

Preparation of normal and diabetic wound models

This study has been reported in line with the ARRIVE guidelines 2.0. All animal experiments were conducted in accordance with the *National Institutes of Health Guide for the Care and Use of Laboratory Animals* and approved by the Biological Research Ethics Committee of the Chinese Academy of Sciences (Ref.no. 2021–B13). Adult male C57BL/6J mice (7–8 weeks old) (Cavens Lab Animals Co., Ltd., China) were housed under specific pathogen-free conditions with a 12/12-hour light/dark cycle. The mice were fed a high-fat diet comprising 60 kcal% fat (FBSH, China) for one week, followed by intraperitoneal injections of streptozotocin (STZ, 50 mg/kg/d; 13104, Cayman, USA) for five consecutive days. Blood glucose levels were monitored every five days using a glucometer (Accu-Chek Performa, Roche Diagnostics, USA). Mice exhibiting blood glucose levels ≥ 16.7 mM for two consecutive weeks were considered diabetic. Control mice were maintained on a standard diet.

To avoid the influence of mice skin contraction, we followed a two-layer patch method [15] for wound preparation and the subsequent transplantation experiments. At the age of 12–13 weeks, mice were depilated, anesthetized with 3% isoflurane (RWD, China) and coated with a 3 cm × 2 cm antibacterial film (REF6640, Drape Antimicrob, 3 M, USA) on the back skin. Two of full-thickness

wounds (Φ = 8 mm) were created by skin biopsy instrument (Honglong, China) within the film area of each mouse. Two wounds were cut with a distance of at least 1 cm to minimize the interference between wounds. After the engrafting experiment, the wounds were covered with another 3 × 2 cm film to keep sterile and prevent skin contraction. Each mouse was raised in separate cages after operation. Each wound was considered an experimental unit to avoid individual and locational differences.

Animal treatment and wound area assessment

The first cohort of mice were divided into two groups: the diabetic mice ($n = 12$) served as the experimental group, and the normal mice ($n = 12$) served as the control group. Neither group received any treatment from the time of wound creation (Day 0, D0) until sacrifice (Day 28, D28). Wound sizes were documented on D0, D7, D14, D21, and D28 post-surgery from a perpendicular viewpoint using a digital camera, and calculated using ImageJ software. The wound tissues were collected for immunostaining and qPCR at D7, D14, D21 and D28, respectively.

Fibrin Glue (FG), formed in situ by mixing fibrinogen and thrombin, was used as a basic scaffold to load MSCs in the present study [15–18]. The second cohort of all diabetic mice ($n = 18$) was randomly (RAND; Microsoft Excel) divided into three groups: (1) control group ($n = 6$), which received 10 μL fibrinogen and 10 μL thrombin per wound; (2) MSC^{GFP} group ($n = 6$), which received a mix of 10 μL fibrinogen containing 1×10^6 MSC^{GFP} cells and 10 μL thrombin per wound; (3) MSC^{ANG1} group ($n = 6$), which received a mix of 10 μL fibrinogen containing 1×10^6 MSC^{ANG1} cells and 10 μL thrombin per wound. All the mice were received transplantation on D0 and D14, and wound sizes were recorded on D0, D7, D14, D21, and D28. The wound tissues were collected for histological staining, qPCR and Western blot at D14 and D28, respectively.

Immunohistochemistry

Mice were euthanized with carbon dioxide. The wound tissues containing both the wound bed and the regenerated surrounding skin (Φ = 8 mm) were harvested. Tissue samples were cut along the midline. Half was used for total RNA or protein extraction; the other half was fixed with 4% paraformaldehyde and then paraffin sectioned (6 μm thickness). Sections were processed for hematoxylin and eosin (H&E) staining or immunofluorescence (IF) staining using the appropriate primary antibodies: anti-GFP (ab13970, Abcam, US), anti-cluster of differentiation 34 (CD34) (ab8158, Abcam, US), anti-Keratin 14 (K14) (ab181595, Abcam, US), anti-K17 (sc-393091, Santa Cruz, USA), anti-alpha-smooth muscle actin (α-SMA) (ab5694, Abcam, US), anti-vascular endothelial cadherin (VE-Cadherin) (ab205336, Abcam, US). Immunoreactivity was visualized using appropriate Alexa Fluor-conjugated secondary antibodies and observed using the confocal microscope (A1R HD25, Nikon, Japan).

Quantitative PCR (q-PCR)

Total RNA from the wounded skin samples (right half) was harvested using Trizol (15596026, Thermo, USA) and quantified using a NanoDrop 2000 (Thermo, USA). The extracted RNA was reverse transcribed with 5 × primerscript RT master mix (R323-01, Vazyme, China). q-PCR was performed on Bio-Rad CFX96 PCR System by using TB Green Premix Taq (RR042B, TAKARA, Japan) and proper primers (Table S1). The housekeeping gene GAPDH served as an internal reference.

Western blot (WB)

Wound tissue (right half) or cells were lysed in cell lysis buffer (P0013, Beyotime, China;). After determining the protein concentration (BCA method), samples were separated on 10-15% polyacrylamide gels and transferred to polyvinylidene difluoride (PVDF) membranes. The membranes were blocked and incubated overnight at 4 °C with primary antibodies against ANG1 (ab183701, Abcam, US), CD34 (ab8158, Abcam, US), Tie2 (53067, SAB, USA), p-Tie2 (13477, SAB, USA), protein kinase B (Akt) (4691 S, CST, USA), p-Akt (4060 S, CST, USA), and VE-Cadherin (ab205336, Abcam, US). Specific protein bands were observed using enhanced chemiluminescence (P0018, Beyotime, China) and quantitatively analyzed using ImageJ software (National Institutes of Health, USA).

Statistical analysis

Numerical data are presented as mean ± SD. Statistical analyses were subjected to unpaired t-tests or analysis of variance (ANOVA) with appropriate post-hoc tests, utilizing GraphPad Prism version 8.0 (GraphPad Software, USA). The level of significance was set at $p < 0.05$.

Results

Reduced angiogenesis and ANG1 levels in the diabetic wound healing

Wound healing in diabetic mice was notably slower compared to normal mice, as evidenced by the larger wound areas observed at 7 days, 14 days, and 21 days post-injury, starting from the same initial wound area (Fig. 1A and B). Consistent with the understanding that angiogenesis plays a pivotal role in the development and outcome of DFU [3], our results revealed a significantly lower presence of vessel-like structures containing CD34-positive hematopoietic and endothelial cells in the regenerated tissue of diabetic wounds compared to normal wounds at 14 days and 28 days post-injury (Fig. 1C and D).

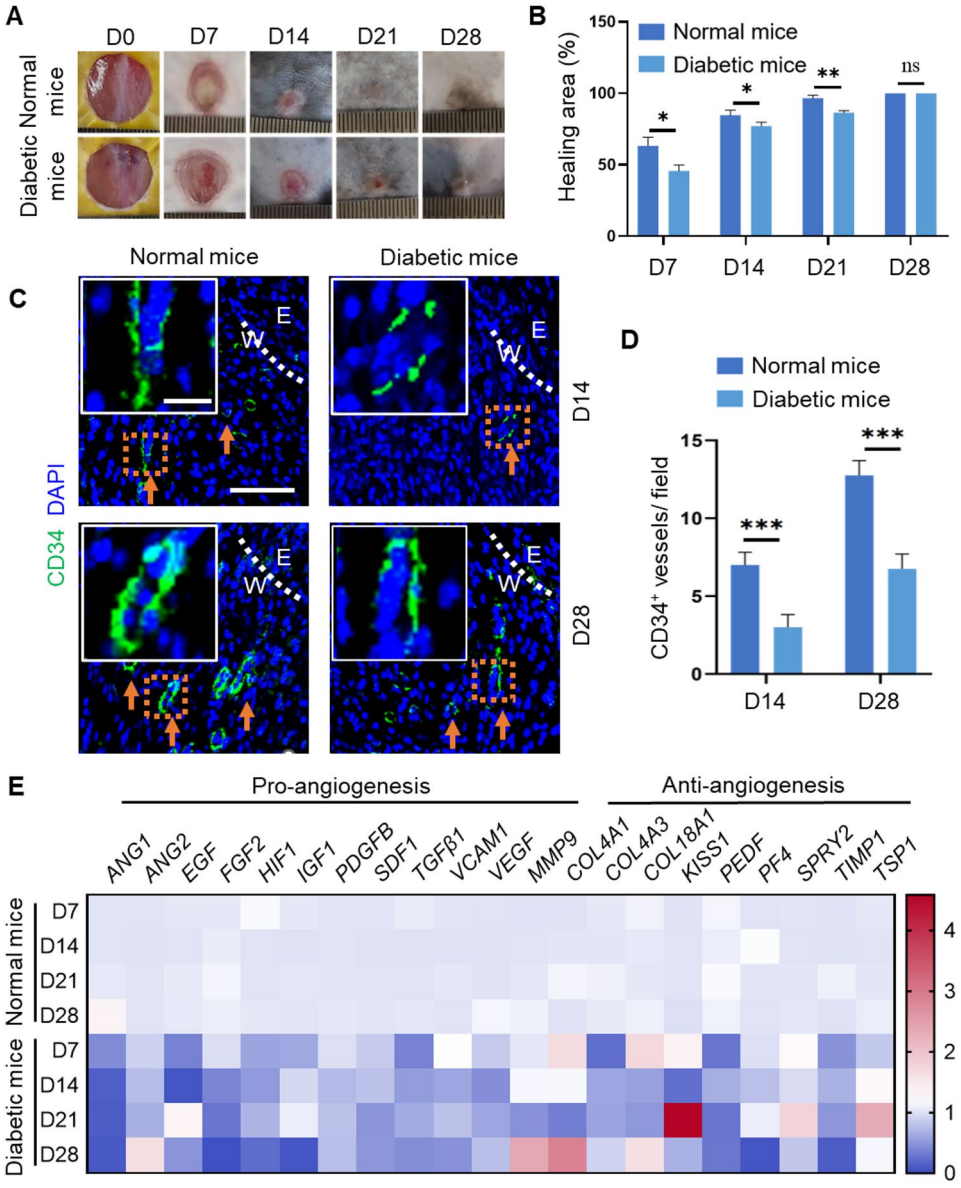

Fig. 1 The impaired ANG1 signaling and angiogenesis in diabetic wound healing. (**A**) A comparison of the wound healing process between normal mice and diabetic mice. (**B**) Quantitative analysis showing the dynamic changes in wound areas during the healing process in normal and diabetic mice. $n = 6$. (**C**) Representative immunostaining images of CD34, a marker of vascular endothelial cells, in normal and diabetic wounds at 14 or 28 days post-wound creation. W, wound central areas and E, wound edges. (**D**) Quantitative analysis of $CD34^+$ vessel-like structures in the wound edge area of diabetic wounds compared to normal wounds. $n = 6$. (**E**) The results of q-PCR revealing the differential expression levels of various molecules regulating angiogenesis on days 7, 14, 21, and 28 during normal and diabetic wound healing. Notably, the expression levels of ANG1 were significantly lower throughout the diabetic wound healing process compared to normal healing. All data are presented as mean ± SD. Scale bar: 100 μm in C and 20 μm in the magnified figure in C. * $p < 0.05$, ** $p < 0.01$, *** $p < 0.001$

These observations suggest inadequate angiogenesis and delayed healing in diabetic wounds relative to normal wounds.

The temporal expression of pro- and anti-angiogenic factors during normal and diabetic wound healing was examined to identify a suitable candidate for engineered MSCs construction. Consistent with the noted reduction in angiogenesis during diabetic wound healing, there was a general trend towards reduced expression levels of pro-angiogenic factors like fibroblast growth factor 2 (FGF2), ANG1, epidermal growth factor (EGF), and the transcription factor hypoxia-inducible factor-1 (HIF1), with concurrent increases in anti-angiogenic factors such as sprouty RTK signaling antagonist 2 (SPRY2), thrombospondin 1 (TSP1), kisspeptin-1 (KISS1), and type IV collagen a1 chain (COL4A1). The interaction between these angiogenic factors in diabetic wound healing is complex, as some pro-angiogenic factors like

matrix metallopeptidase 9 (MMP9) were upregulated, while anti-angiogenic factors like tissue inhibitor of matrix metalloprotease 1 (TIMP1) and platelet factor 4 (PF4) were down-regulated in the later stages of diabetic wound healing compared to normal healing (Fig. 1E). Given the intricate interplay of pro- and anti-angiogenic factors during angiogenesis, the expression levels of these factors displayed dynamic and varied changes throughout the healing process. Notably, the consistently reduced expression of the pro-angiogenic factor ANG1 across the entire diabetic wound healing process (Fig. 1E) suggests that ANG1 may serve as a crucial therapeutic target to enhance inadequate angiogenesis and represents an optimal candidate for constructing engineered MSCs for diabetic wound healing applications.

Construction of trackable MSCs stably expressing ANG1

A lentiviral plasmid containing both *ANG1* and *GFP* genes linked via a *t2A* linker was designed and constructed (Fig. 2A), and the lentiviral infected MSCs (MSC^{ANG1}) were evaluated for the stable expression of these two exogeneous proteins. Immunostaining for GFP indicated that MSC^{ANG1} exhibited comparable GFP fluorescence levels to MSCs infected with a GFP lentivirus (MSC^{GFP}) (Fig. 2B and C). The average proportion of GFP-expressing cells within the MSC^{ANG1} and MSC^{GFP} populations was approximately 80% (Fig. 2B and C), indicating that the engineered MSCs expressed exogenous genes robustly and were suitable for subsequent experiments.

Flow cytometry analysis revealed that MSC^{ANG1} and untreated MSC shared similar expression profiles;

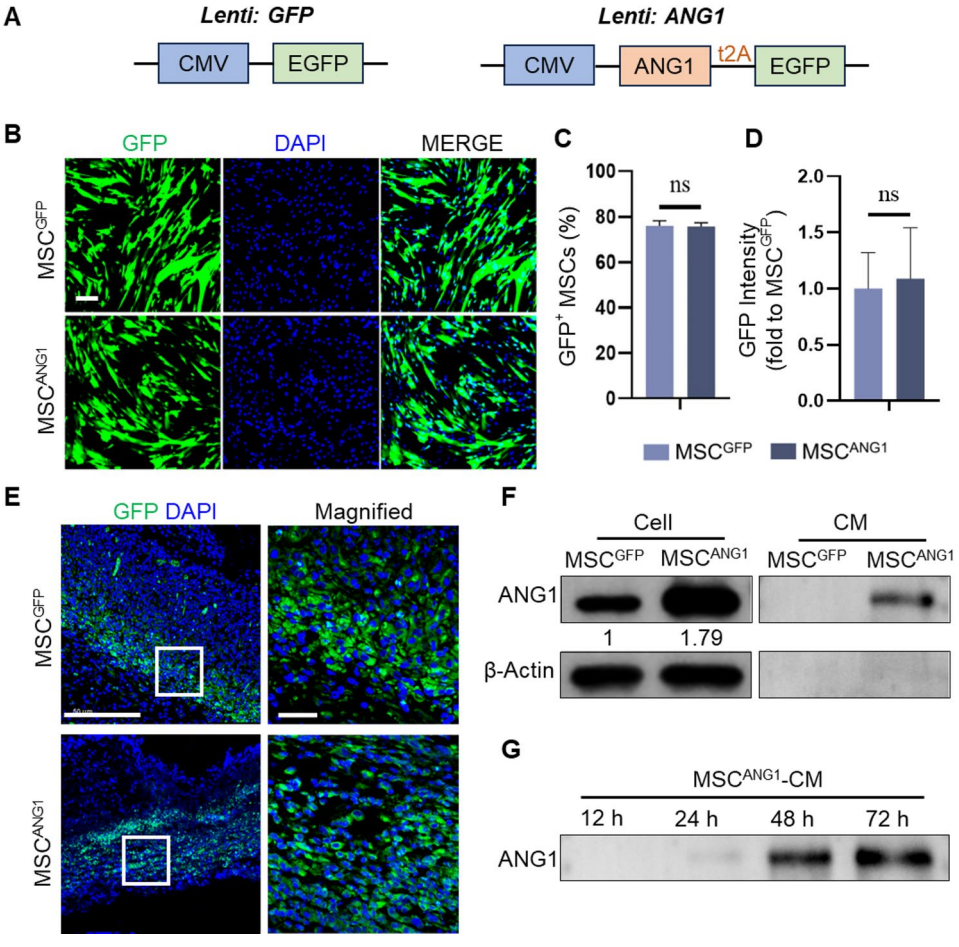

Fig. 2 Construction and characterization of engineered MSCs stably expressing ANG1 (MSC^{ANG1}). (**A**) Schematic illustration of the lentiviral plasmids carrying GFP, or both ANG1 and GFP. (**B**) Representative immunostaining images of GFP showing the presence of GFP in MSCs infected with GFP (MSC^{GFP}) and ANG1 (MSC^{ANG1}) lentivirus. (**C**) Quantitative analysis of GFP intensity in MSC^{GFP} and MSC^{ANG1}. $n=6$. (**D**) Statistical analysis of GFP intensity in the diabetic wounds engrafted with MSC^{GFP} and MSC^{ANG1} for 7 days. (**E**) Representative images of GFP immunostaining showing the survival of MSC^{GFP} or MSC^{ANG1} engrafted onto the diabetic wounds for 7 days. The areas in the white boxes were enlarged and shown in the right panel. (**F**) WB showed the expression levels of ANG1 in MSC^{ANG1} and MSC^{GFP}, as well as the levels in CM of MSC^{ANG1} and MSC^{GFP}. Full-length blots are presented in Fig. S3 (**G**) WB showed the expression levels of ANG1 in CM of MSC^{ANG1} cultured for 12 h, 24 h, 48 h, and 72 h, respectively. Full-length blots are presented in Fig. S3. Scale bar: 50 μm in B, 100 μm in left panel of D and 20 μm in right panel of D. All data are presented as mean ± SD

they both expressed high levels of mesenchymal-specific markers such as CD90 and CD105, and did not express the hematopoietic marker CD34 and the leukocyte marker CD45 (Fig. S1A). Furthermore, MSC^{ANG1} retained their ability to differentiate into osteognic (Fig. S1B) and adipogenic (Fig. S1C) lineages under specific induction conditions. WB analysis revealed a substantial increase in ANG1 expression levels in the lysate and CM of MSC^{ANG1} cells compared to MSC^{GFP} cells (Fig. 2F), confirming the successful expression and secretion of the angiogenic factor ANG1. The content of ANG1 in the CM of engineered MSCs exhibited a temporal increase, further confirming that ANG1 protein was released from MSC^{ANG1} cells and gradually accmulated in the CM. (Fig. 2G).

Subsequently, we examined the impact of ANG1 on the survival of transplanted engineered MSCs in diabetic wounds. By tracking the transplanted cells using GFP immunostaining, we observed that MSC^{ANG1} exhibited a similar survival pattern to MSC^{GFP} cells 7 days after transplantation into the diabetic wounds (Fig. 2D and E). This indicated that ANG1 production in MSCs did not affect the in vivo survival of MSCs.

MSCANG1 promoted survival, tubulogenesis as well as akt activation of HUVECs

Considering that MSCs exert their therapeutic effects primarily through paracrine mechanisms, we evaluated the impact of MSC^{ANG1} on endothelial cells by treating HUVECs with CM from various engineered MSCs. MSC^{GFP} displayed moderate protective effects on the survival of HUVECs, as indicated by significantly increased cell number (Fig. 3A) and fewer apoptotic cells positive for both Annexin V and PI in HUVECs treated with MSC^{GFP}-CM compared to the Ctrl group (Fig. 3B and C). Moreover, MSC^{ANG1}-CM further enhanced the survival of HUVECs in comparison to MSC^{GFP}-CM, underscoring the synergistic effects of ANG1 and MSCs on the survival of endothelial cells (Fig. 3A-C). Such effects were confirmed through calcein-AM and PI staining. HUVECs treated with MSC^{ANG1}-CM exhibited a significantly higher number of Calcein-AM-stained live cells and fewer PI-stained dead cells as compared to either Ctrl- or MSC^{GFP}-CM-treated ones (Fig. 3D-F). The application of ANG1 protein produced similar protective effects on the survival of HUVECs (Fig. S2), further highlighting the protective role of ANG1. Endothelial cells possess the capability to form capillary-like structures in vitro, reflecting their angiogenic potential in vivo. Similarly, treatment with MSC^{GFP}-CM enhanced the formation of capillary-like structures in HUVECs, and this effect was further significantly amplified with MSC^{ANG1}-CM treatment (Fig. 3G and H).

The Akt pathway is closely associated with the survival and angiogenic capacity of endothelial cells. Through WB analysis, we observed increased phosphorylation and activation of Tie2, the specific receptor of ANG1 on endothelial cells, in HUVECs treated with MSC^{ANG1}-CM compared to Ctrl and MSC^{GFP}-CM-treated ones (Fig. 3I and J). Additionally, elevated Akt phosphorylation levels were observed in MSC^{ANG1}-CM-treated HUVECs, providing evidence that MSC^{ANG1} significantly enhanced Akt activation *via* the Tie2 (Fig. 3I and J). It is noteworthy that HUVECs treated with MSC^{GFP}-CM also exhibited slight activation of Tie2 and Akt proteins, aligning with the observation that MSC^{GFP}-CM modestly improved the survival and angiogenic capacity of endothelial cells.

MSCANG1 promoted functional maturation of HUVECs

ANG1 plays a pivotal role in vascular stabilization and structural integrity during the angiogenesis process [19]. To assess the impact of engineered MSCs on endothelial cell integrity, HUVECs were cultured with CM from the engineered MSCs, and the permeability of the HUVECs monolayer was evaluated by quantifying the fluorescent dye Dextran-FITC that penetrated through the cells (Fig. 4A). Notably, HUVECs incubated with MSC^{ANG1}-CM exhibited significantly reduced Dextran-FITC penetration compared to both Ctrl and MSC^{GFP}-CM incubated HUVECs (Fig. 4B), indicating that ANG1 effectively decreased endothelial barrier leakage, thereby promoting vascular integrity.

VE-Cadherin, a critical component of endothelial cell-to-cell adherent junctions responsible for calcium-dependent cell adhesion, plays a key role in maintaining vascular integrity [20]. Our observations revealed an upregulation in VE-cadherin expression at the cell border of HUVECs following incubation with MSC^{ANG1}-CM, in contrast to Ctrl and MSC^{GFP}-CM-treated HUVECs (Fig. 4C and D). WB analysis also demonstrated the significantly enriched VE-cadherin expression in these MSC^{ANG}-CM treated HUVECs (Fig. 4E and F). Furthermore, the phosphorylation of proto-oncogene tyrosine-protein kinase Src (Src) has been associated with reduced VE-cadherin stability at cell junctions [21]. MSC^{ANG1}-CM treatment led to reduced levels of phosphorylated Src in HUVECs compared to the Ctrl and MSC^{GFP}-CM treatment (Fig. 4E and F).

In line with previous findings suggesting that naive MSCs possess some angiogenic potential, we observed that MSC^{GFP}-CM treatment also modestly improved permeability, increased VE-cadherin expression, and reduced Src phosphorylation in HUVECs (Fig. 4A-F). Overall, exogenous ANG1 expression in MSCs is shown to further enhance their angiogenic capacity by promoting the functional maturation of endothelial cells.

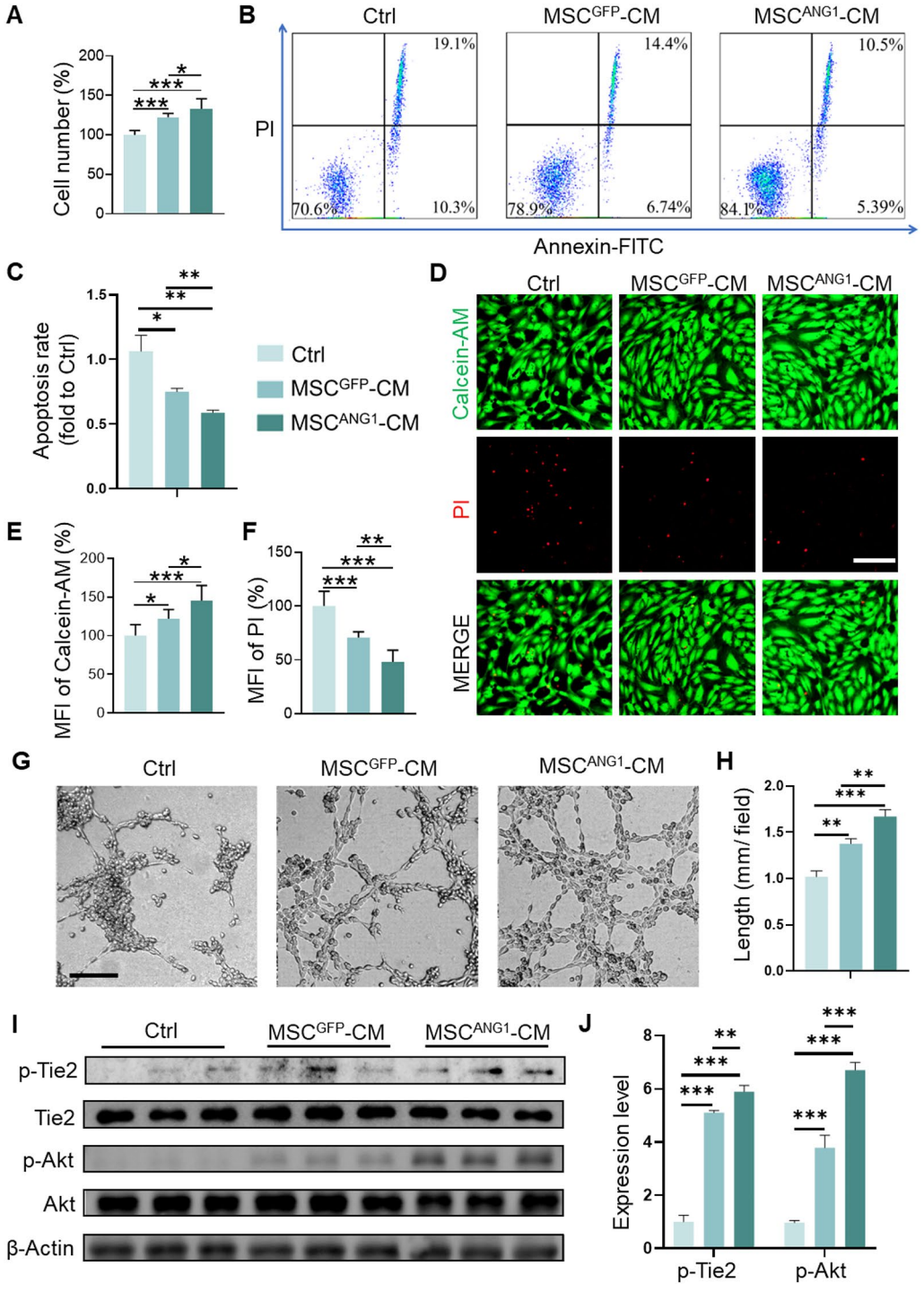

Fig. 3 MSC ^{ANG1} promoted the survival, tubulogenesis and Akt activation in HUVECs. (**A**) CCK8 assay showing the total number of HUVECs treated with Ctrl, MSC^{GFP}-CM, and MSC^{ANG1}-CM for 48 h. $n=6$. (**B**) Flow cytometry of PI and Annexin-V in HUVECs treated with Ctrl, MSC^{GFP}-CM or MSC^{ANG1}-CM for 48 h. (**C**) Statistical analysis of apoptosis (PI^{+}/Annexin-V^{+}) in HUVECs treated with Ctrl, MSC^{GFP}-CM or MSC^{ANG1}-CM for 48 h. $n=3$. (**D**) Representative images of Calcein-AM and PI staining, illustrating HUVECs treated with Ctrl, MSC^{GFP}-CM, or MSC^{ANG1}-CM for 48 h. (**E** and **F**) Statistical analysis of the mean fluorescence intensity (MFI) for Calcein-AM (**E**) and PI (**F**). $n=6$. (**G**) Representative images showing the tube formation of HUVECs treated with Ctrl, MSC^{GFP}-CM, and MSC^{ANG1}-CM for 4 h. (**H**) Quantitative analysis of the length of tubes in HUVECs. $n=9$. (**I**) Representative WB images of p-Tie2, Tie2, p-Akt and Akt expression levels in HUVECs after treatment with Ctrl, MSC^{GFP}-CM, and MSC^{ANG1}-CM for 48 h. β-Actin was the internal control. Full-length blots are presented in Fig. S3. (**J**) Semi-quantitative analysis of the phosphorylation of Tie2 (p-Tie2/Tie2) and Akt (p-Akt/Akt) in HUVECs. $n=9$. Scale bar: 100 μm in C. All data are presented as mean ± SD. $_{*}p<0.05$, $_{**}p<0.01$, $_{***}p<0.001$

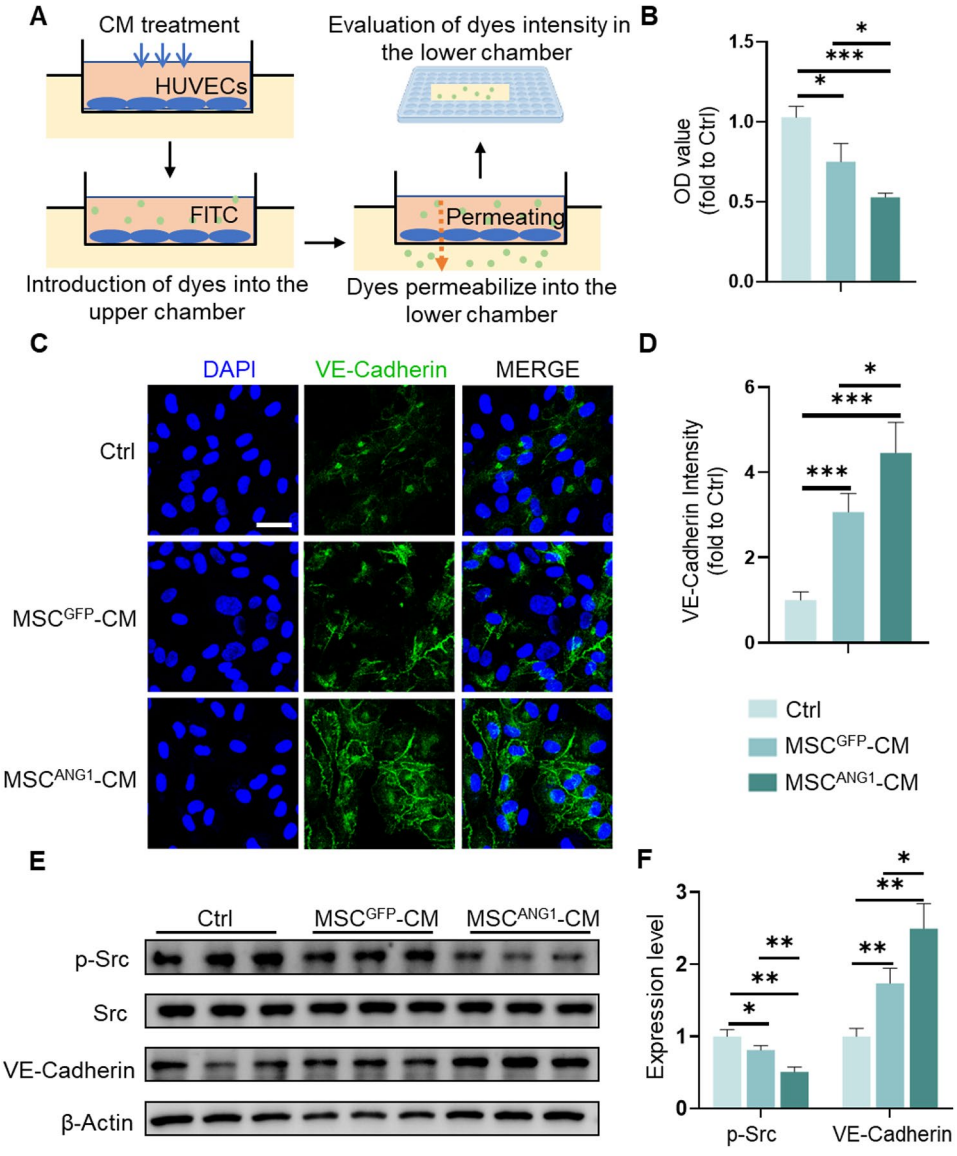

Fig. 4 MSC ^{ANG1}promoted VE-Cadherin expression, vascular integrity, and inhibited Src activation. (**A**) Schematic diagram illustrating the evaluation of endothelial barrier integrity. (**B**) Statistical analysis of the fluorescence intensity of FITC-Dextran that permeated through the monolayer of HUVECs treated with Ctrl, MSC^{GFP}-CM, or MSC^{ANG1}-CM for 48 h. $n = 3$. (**C**) Representative immunostaining images of VE-Cadherin in HUVECs following treatment with Ctrl, MSC^{GFP}-CM, and MSC^{ANG1}-CM for 48 h. (**D**) Quantitative analysis of VE-Cadherin fluorescence intensity in HUVECs post-treatment. $n = 9$. (**E**) Representative WB images depicting the expression levels of p-Src, Src, and VE-Cadherin in HUVECs after treatment with Ctrl, MSC^{GFP}-CM, and MSC^{ANG1}-CM for 48 h. β-Actin served as the internal control. Full-length blots are presented in Fig. S3. (**F**) Semi-quantitative analysis of Src phosphorylation levels (p-Src/Src) and VE-Cadherin expression in HUVECs. $n = 9$. Scale bar: 50 μm in C. All data are presented as mean ± SD. $_{*}p < 0.05$, $_{**}p < 0.01$, $_{***}p < 0.001$

MSCANG1 engraftment promoted angiogenesis in diabetic wound healing

The angiogenesis in diabetic wound healing post-engraftment with various engineered MSCs was evaluated by examining both the presence and maturation of vasculature 14 days after transplantation. Double immunostaining for CD34 and α-SMA, a pericyte marker, demonstrated a notable increase in vessel-like structures characterized by CD34^{+} cells in the inner layer and α-SMA^{+} cells in the outer layer in the wound tissues transplanted with MSC^{ANG1}, in comparison to the control and those transplanted with MSC^{GFP} (Fig. 5A and B). WB analysis further confirmed elevated CD34 expression in the regenerated wound tissue from MSC^{ANG1}-transplanted diabetic wounds (Fig. 5C and D).

Multiple molecular signaling pathways involved in the wound healing process ultimately converge on the activation of Akt, with impaired Akt activation commonly observed in diabetic wound healing [22, 23]. In the present study, WB analysis revealed significant phosphorylation of the Tie2 receptor and downstream Akt pathways in MSC^{ANG1}-transplanted diabetic wounds (Fig. 5E and

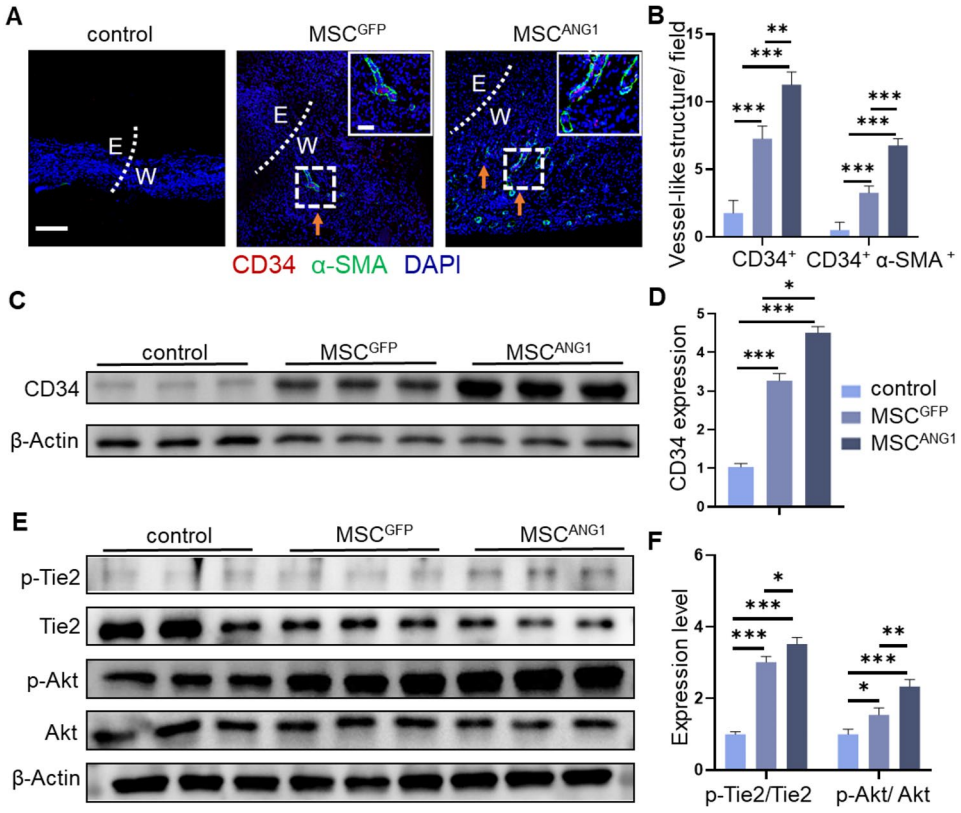

Fig. 5 MSC ^{ANG1} promoted angiogenesis and activated Tie2/Akt pathway in diabetic wound healing. (**A**) Representative images of double staining for CD34 and αSMA in the diabetic wounds treated with control, MSC^{GFP}, and MSC^{ANG1} for 14 days. W, the center area of wounds, and E, the transitional area of wounds. The area in the dashed box was enlarged and shown in the insets. Arrows indicated the vessel-like structure positive for both CD34 and αSMA. (**B**) Quantitative analysis of the vessel-like structures positive for CD34, or CD34 and αSMA. $n=6$. (**C**) Representative WB image revealing the expression levels of CD34 in diabetic wounds treated with control, MSC^{GFP}, and MSC^{ANG1} for 14 days. β-Actin was set as the internal control. Full-length blots are presented in Fig. S3. (**D**) Semi-quantitative analysis of CD34 expression in diabetic wounds. $n=9$. (**E**) Representative WB images of p-Tie2, Tie2, p-Akt and Akt expression levels in diabetic wounds treated with control, MSC^{GFP}, and MSC^{ANG1} for 14 days. β-Actin was set as the internal control. Full-length blots are presented in Fig. S3. (**F**) Semi-quantitative analysis of the phosphorylation of Tie2 (p-Tie2/Tie2) and Akt (p-Akt/Akt) in the diabetic wound healing. $n=9$. Scale bar: 100 μm in A, 20 μm in the insert panel of A. All data are presented as mean ± SD. $*p<0.05$, $**p<0.01$, $***p<0.001$

F), suggesting that the activation of the ANG1/Tie2/Akt pathway contributes to the angiogenic mechanism underlying MSC^{ANG1}-enhanced angiogenesis in diabetic wound healing.

The expression of the inter-endothelial junction protein VE-Cadherin was examined to assess the integrity and maturation of vasculature in the regenerated wound tissues. Immunostaining for CD34 and VE-Cadherin revealed that wounds treated with MSC^{ANG1} exhibited a significantly higher presence of vessel-like structures positive for both CD34 and VE-Cadherin, as compared to those treated with control and MSC^{GFP} (Fig. 6A and B). The elevated expression of VE-Cadherin in MSC^{ANG1}-treated wounds was further validated through WB analysis (Fig. 6C and D). Additionally, WB analysis revealed a reduction in Src expression in MSC^{ANG1}-treated wounds when compared to those treated with control and MSC^{GFP} (Fig. 6C and D). These findings suggest that MSC^{ANG1} effectively suppressed Src activity, thereby promoting the expression of its downstream effector, VE-Cadherin.

Taken together, these results indicate that MSC^{ANG1} treatment significantly activates the Akt pathway and inhibits Src activity through binding to the Tie2 receptor, resulting in enhanced angiogenesis and improved vascular integrity during diabetic wound healing.

MSCANG1 engraftment accelerated diabetic wound healing

We proceeded to investigate whether MSC^{ANG1} engraftment could enhance the process of diabetic wound healing. Consistent with the observed promotion of angiogenesis in the wound tissues by MSC^{ANG1}, the wound areas engrafted with MSC^{ANG1} exhibited significantly smaller sizes compared to those engrafted with control or MSC^{GFP} at 7, 14, and 21 days post-engraftment (Fig. 7A and B). These findings indicate that engineered MSC^{ANG1} can significantly expedite wound healing.

Epithelial recovery is crucial for reestablishing the wound barrier, a critical event of the wound healing process [24]. Utilizing Hematoxylin and Eosin (HE)

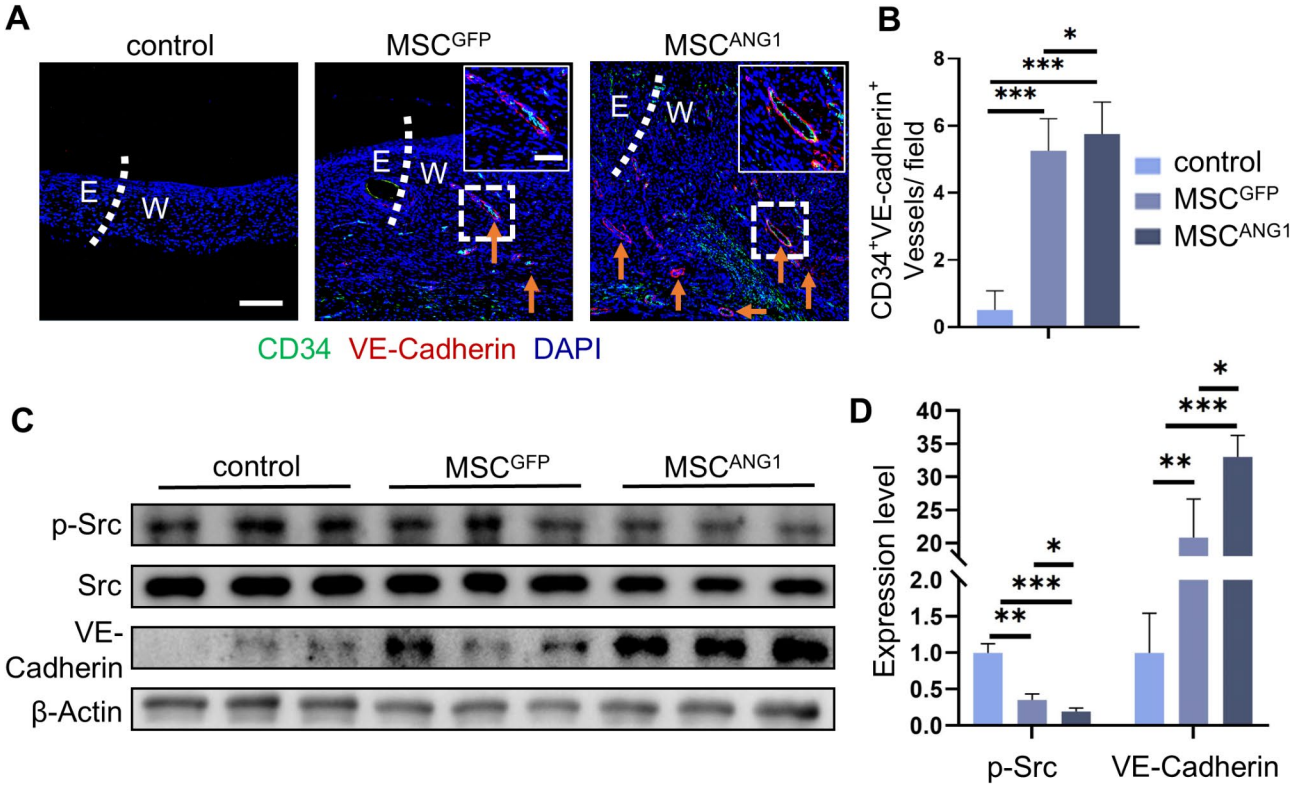

Fig. 6 MSC ^{ANG1} promoted the VE-Cadherin expression and inhibited Src activation in diabetic wound healing. (**A**) Representative images of double staining for CD34 and VE-Cadherin in the diabetic wounds treated with control, MSC^{GFP}, and MSC^{ANG1} for 14 days. W, the center area of wounds, and E, the transitional area of wounds. The area in the dashed box was enlarged and shown in the insets. Arrows indicated the vessel-like structures positive for both CD34 and VE-Cadherin. (**B**) Quantitative analysis of vessel-like structure positive for both CD34 and VE-Cadherin in diabetic wounds. $n=6$. (**C**) Representative WB images showing the expression levels of p-Src, Src VE-Cadherin in diabetic wounds treated with control, MSC^{GFP}, and MSC^{ANG1} for 14 days. β-Actin served as the internal reference. Full-length blots are presented in Fig. S3. (**D**) Semi-quantitative analysis of Src activation (p-Src/Src) and VE-Cadherin expression levels in the diabetic wounds. $n=9$. Scale bar: 100 μm in A, 20 μm in the insert panel of A. All data are presented as mean ± SD. $*p<0.05$, $**p<0.01$, $***p<0.001$

staining and immunostaining against K14, an epithelial marker, we observed that diabetic wounds engrafted with MSC^{ANG1} displayed the narrowest epithelial gap (EG) at 14 days post-engraftment compared to those engrafted with control and MSC^{GFP} (Fig. 7C, D, and F). By the 28th day post-transplantation, all wounds were epithelium-covered, with significantly increased dermal thickness (THK) in the wounds engrafted with MSC^{GFP} and MSC^{ANG1} compared to the control (Fig. 7C, D, and G). Notably, the dermal thickness in the wounds engrafted with MSC^{GFP} and MSC^{ANG1} showed no significant disparity (Fig. 7C and G), suggesting that MSC^{ANG1} treatment did not induce excessive proliferative effects on dermal fibroblasts.

Angiogenesis plays a pivotal role in the functional regeneration of skin appendages [25]. Through double immunostaining for K14 and K17, a marker of the regenerated hair follicles, we observed a higher number of K14- and K17-colocalized hair follicles in the transitional region of diabetic wounds at both 14 and 28 days post-engraftment following MSC^{ANG1} transplantation (Fig. 7E and H). Altogether, these findings suggest that MSC^{ANG1} accelerates diabetic wound healing by facilitating epidermal and dermal reconstruction, as well as promoting skin appendage regeneration.

Discussion

Inadequate blood flow and compromised circulation are significant hurdles in the healing of diabetic skin ulcers, highlighting the importance of boosting angiogenesis and enhancing blood perfusion in diabetic wound care. Our study reveals that treatment with MSCs alone promotes angiogenesis and facilitates the healing of diabetic foot ulcers, while the engineering of MSCs with ANG1 provides additional benefits to this therapeutic process. Together, these treatments offer a promising avenue for the development of novel strategies in the management and prevention of diabetic foot ulcers.

Angiogenesis is a critical process essential for the formation of granulation tissue, a key milestone in wound healing [26]. The intricate orchestration of angiogenic events relies on a delicate equilibrium between various

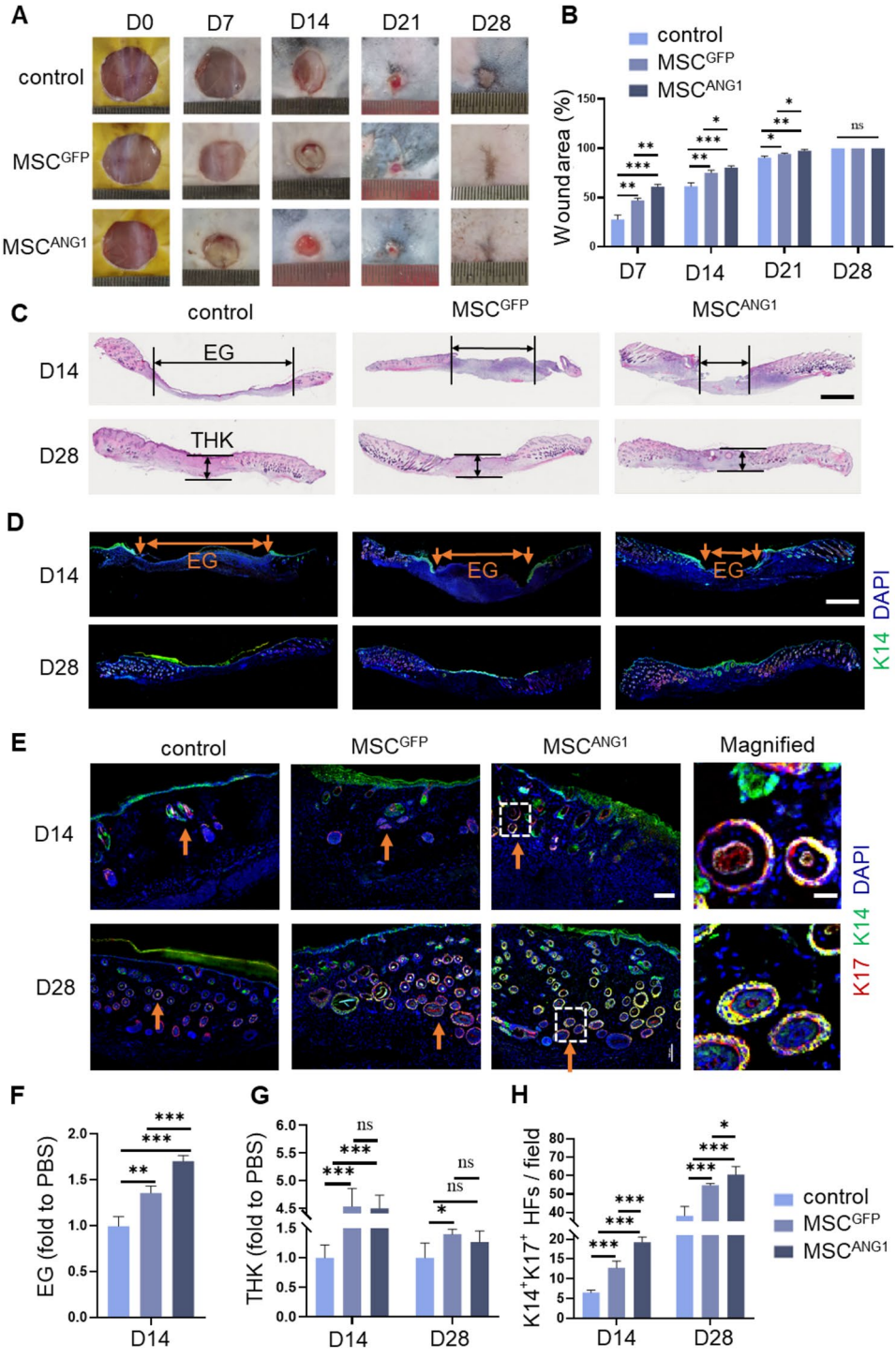

Fig. 7 (See legend on next page.)

pro- and anti-angiogenic factors. Upon injury, local microvascular disruption-induced hypoxia triggers the activation of HIF-1α, which stimulates angiogenesis through diverse mechanisms including the production of key angiogenic growth factors such as vascular endothelial growth factor (VEGF-A), stromal cell-derived factor-1 (SDF-1) and so on [27, 28]. Subsequent to the peak in vessel density, an upregulation of anti-angiogenic factors including Sprouty2 and pigment epithelium-derived factor (PEDF) ensues, leading to the regression of the vascular network [29, 30]. The maturation of the vascular network necessitates the stabilization of capillaries by pericytes and vascular smooth muscle cells (vSMCs) [31], and platelet-derived growth factor-BB (PDGF-BB) plays

(See figure on previous page.)

Fig. 7 MSC ^{ANG1} treatment promoted diabetic wound healing process. (**A**) Representative images displaying the dynamic changes in skin wounds of diabetic mice treated with control, MSC^{GFP}, and MSC^{ANG1}. (**B**) MSC^{ANG1} treatment resulted in a substantial reduction in wound area in diabetic mice models at various time points compared to control and MSC^{GFP} treatment. The percentage of wound healing area was calculated as 100% × (initial wound area - wound area at different time points) / initial wound area. $n = 6$. (**C**) Hematoxylin and Eosin (H&E) staining of diabetic wounds transplanted with control, MSC^{GFP}, and MSC^{ANG1} for 14 and 28 days, respectively. (**D**) Representative immunostaining images of K14 in diabetic wounds transplanted with control, MSC^{GFP}, and MSC^{ANG1} for 14 and 28 days, respectively. The epithelial gap (EG) signifies the area of the wound that remained uncovered by the K14-positive epidermis. (**F**) Representative images of double immunostaining for K14 and K17 in diabetic wounds transplanted with control, MSC^{GFP}, and MSC^{ANG1} for 14 and 28 days, respectively. The area within the dashed box was magnified and presented in the right panel. Arrows indicate hair follicles positive for both K14 and K17. (**F**) Statistical analysis indicating that MSC^{ANG1}-treated diabetic wounds depicted a notably reduced EG compared to the control or MSC^{GFP}-treated wounds. $n = 6$. (**G**) Statistical analysis illustrating that MSC^{ANG1} and MSC^{GFP}-treated wounds exhibited significantly increased dermal thickness (THK) of the regenerated tissues compared to the control. THK was defined as the dermal thickness in the central area of the regenerated tissues. $n = 6$. (**H**) Statistical analysis demonstrating that MSC^{ANG1}-treated diabetic wounds displayed significantly more hair follicles positive for both K14 and K17 compared to the control and MSC^{GFP}-treated wounds. $n = 6$. Scale bar: 1 mm in C and D, 100 μm in the left three panel of E and 20 μm in the right panel of E. All data are presented as mean ± SD. * $p < 0.05$, ** $p < 0.01$, *** $p < 0.001$

a crucial role in the pericyte recruitment and differentiation [32]. Furthermore, the intricate interplay of ANG1 and Angiopoietin-2 (ANG2) in conjunction with the receptor Tie2 intricately regulate angiogenesis and vascular network maturity [33]. This intricate regulation highlights the complexity of diabetes-impaired angiogenesis in the wound healing process. In our study, we conducted a thorough comparison of the expression levels of various pro- and anti-angiogenic factors and identified ANG1 as likely the most affected and impaired angiogenic factor in the healing of DFU, suggesting ANG1 as a potential innovative target for addressing impaired angiogenesis during diabetic wound healing. Consistent with our observations, previous research has indicated a decreased ANG1 to ANG2 ratio in diabetic wounds, indicating a disruption in the diabetic wound angiogenesis to progress towards a mature phenotype [34, 35].

Many studies have explored the use of ANG1 for wound treatment. In experiments involving STZ-induced diabetic wounds, adenoviral-mediated overexpression of ANG1 resulted in an increase in endothelial progenitor cells (EPCs) and enhanced neovascularization by day 7 post-injury [36]. With the discovery of MSCs, these cells have emerged as superior candidates for delivering exogenous ANG1 to therapeutic sites due to their potent immunoregulatory and pro-regenerative capabilities, as well as their stability in integrating and expressing exogenous genes [37]. MSCs can be isolated from various tissues, including bone marrow [38], adipose tissue [39], amniotic fluid [40], and umbilical cord [15], etc. In the current study, umbilical cord-derived MSCs were chosen due to their high yield, purity, and low rates of senescence [41].

In our study, it was found that the modification with ANG1 had an insignificant impact on the mesenchymal characteristics and survival after engraftment; however, it altered the release pattern of MSCs, thereby facilitating the formation of a functional vasculature both in vitro and in vivo. As widely reported in literature, the therapeutic efficacy of MSCs primarily derived from their paracrine effects [42]. The regenerative potential of MSCs-releasing factors has been attributed to a complex interplay of various DNA, microRNAs, proteins, cytokines, and membrane lipids, etc [43]. Certain cargo molecules in MSC-derived exosomes have been identified to govern the functional activities of endothelial cells; for instance, proteins like VEGF and ANG2, and microRNAs such as miR-30b and miR-126, play pivotal roles in regulating endothelial cell proliferation, migration, and angiogenesis [43]. These findings are in line with our observation that MSCs alone demonstrate pro-angiogenic effects in DFU healing. Particularly, the inclusion of ANG1 in the MSCs release profile exhibited an additional impact on angiogenesis in DFU healing, specifically contributing to the maturation and stabilization of capillaries.

The underlying signaling pathways in MSC^{ANG1}-promoted DFU healing have also been investigated. The phosphatidylinositol 3-kinase (PI3K)/Akt/mammalian target of rapamycin (mTOR) pathway is known to play a pivotal role in various cellular functions including proliferation, adhesion, migration, invasion, metabolism, survival, as well as the angiogenesis under normal and pathological conditions [44–46]. Activation of the Akt pathway by various pro-angiogenic factors, including VEGF, nitric oxide, and ANG, not only stimulates downstream pathways but also regulates the secretion and expression of these crucial angiogenic factors [44]. Apart from Akt, Src activity is well known for its contributions to the vascular leakage [47]. Src-mediated degradation of VE-cadherin has been identified as a factor contributing to endothelial barrier breakdown under pathological conditions [48, 49]. Studies have indicated that sustained activation of ANG1 can activate Akt, thereby restoring Src activity to basal levels and protecting the endothelial barrier [50]. Furthermore, the Akt and Src pathways are dysregulated in diabetic wounds, making them potential therapeutic targets for enhancing angiogenesis and promoting diabetic wound healing [51, 52]. The observed increase in Akt phosphorylation and inhibition of Src activity further validates the establishment of an effective vasculature in MSC^{ANG1}-treated diabetic wounds.

Enhanced angiogenesis resulting from MSC^{ANG1} treatment in diabetic wounds has shown significant improvements in wound healing outcomes. At 14 days post-injury, MSC^{ANG1}-treated wounds displayed notable advancements in epithelialization and dermal reconstitution, with no excessive dermal proliferation observed by day 28, confirming the positive impact of ANG1-engineered MSCs on wound healing. Recent studies have showed the mutualistic cellular crosstalk between hair follicles and blood vessels [53], where angiogenesis controls hair growth and follicle sizes [25]. Our findings align with this, as MSC^{ANG1}-treated wounds demonstrated enhanced hair follicle regeneration. During normal wound healing, ANG1-engineered MSCs has been reported to promote the development of a more mature and stable vasculature, leading to improved therapeutic outcomes [8]. Our study further highlighted the synergistic effects of MSCs and ANG1 in enhancing angiogenesis and faciliating functional recovery in challenging pathological conditions like DFU.

Collectively, our finding has demonstrated that ANG1 signaling is compromised in the context of diabetic wound healing, and the treatment involving the engineering of MSCs with ANG1 has shown additional therapeutic benefits by enhancing the angiogenic process. While this discovery introduces a novel therapeutic strategy for addressing wounds in diabetic patients, it has been noted that the intricate multi-domain structure of native human ANG1 limits its widespread therapeutic application. The future advancement of more precisely engineered variants, such as cartilage oligomeric matrix protein-angiopoietin-1 (COMP-ANG1), which exhibits a more potent activation of the Tie2 pathway, holds the potential for achieving enhanced therapeutic outcomes [54].

Conclusion

Our findings revealed a notable deficiency in ANG1 during the diabetic wound healing process. Through the construction of trackable engineered MSCs that express the angiogenic factor ANG1 (MSC^{ANG1}), it was observed that MSC^{ANG1} had a noteworthy impact on the survival, migration, and formation of functional tight junctions in endothelial cells. Additionally, MSC^{ANG1} was demonstrated to promote angiogenesis and enhance vascular integrity in diabetic wound healing. The activation of Akt and the inhibition of Src activity were key players in the underlying mechanism of MSC^{ANG1}-induced angiogenesis. In line with the increased angiogenesis, epidermal and dermal reconstruction, as well as hair follicle regeneration, were significantly accelerated in MSC^{ANG1}-treated diabetic wounds as compared to MSC-treated ones. Collectively, the engineering of MSCs with ANG1 provides substantial synergistic advantages for therapeutic outcomes, and offers a promising avenue for developing innovative strategies in the management of DFU.

Abbreviations

αSMA	Alpha smooth muscle actin
Akt	Protein kinase B
ANG1	Angiopoietin-1
ANG2	Angiopoietin-2
CD34	Hematopoietic marker cluster of differentiation
COL4a1	Type IV collagen a1 chain
EGF	Epidermal growth factor
FGF2	Fibroblast growth factor 2
K14	Keratin 14
K17	Keratin 17
HIF1	Hypoxia-inducible factor-1
HUVECs	Human umbilical cord vein endothelial cells
KISS1	Kisspeptin-1
MMP9	Matrix metallopeptidase 9
MSCs	Mesenchymal stem cells
PEDF	Pigment epithelium-derived factor
PF4	Platelet factor 4
SDF-1	Stromal cell-derived factor-1
SPRY2	Sprouty RTK signaling antagonist 2
Src	Proto-oncogene tyrosine-protein kinase Src
Tie2	Angiopoietin-Tie receptor 2
TIMP1	Tissue inhibitor of matrix metalloprotease 1
TSP1	Thrombospondin 1
VE-Cadherin	Anti-vascular endothelial cadherin
VEGF	Vascular endothelial growth factor

Supplementary Information

The online version contains supplementary material available at https://doi.org/10.1186/s13287-025-04207-7 .

Supplementary Material 1

Acknowledgements

The authors declare that they have not used Artifcial Intelligence in this study.

Author contributions

QD, FD: Conceptualization, Methodology, Validation, Data curation, Formal analysis, Writing - Original draft preparation. SP: Methodology, Investigation, Validation, Data curation. YX, YZ: Investigation, Validation. JZ, CL, SY: Writing - Review & Editing, Supervision, Funding acquisition.

Funding

This work was funded by National Key Research and Development Program of China (No. 2021YFA1101100); National Key Research and Development Program of China (No. 2022YFA1104800); National Natural Science Foundation of China (No. 82271522); the Natural Science Foundation of Jiangsu Province (No. BK20243003); Basic Research Program of Suzhou (No. SSD2024019).

Data availability

The data that support the findings of this study are available from the corresponding author upon reasonable request.

Declarations

Ethics approval and consent to participate

Animal experiments: (1) Animal experiment for the efficacy of mesenchymal stem cells in diabetic wound healing. (2) The Ethics Committee for Experimental Animals of Suzhou Institute of Biomedical Engineering Technology, Chinese Academy of Sciences. (3) 2021 – B13. (4) 16/3/2021. The protocols for animal experiments adhere to the ARRIVE (Animal Research: Reporting of in Vivo Experiments) guidelines. Human sample: (1) Fresh MSCs of human was obtained from donors for effectiveness of stem cell therapy. (2)

The Ethics Committee of the First Affiliated Hospital of Soochow University. (3) 2019 – 136. (4) 30/12/2019. Patient provided written informed consent for the use of samples. Human MSCs were isolated from donated human umbilical cord after obtaining permission for their use in research applications by informed consent or legal authorization

Consent for publication
Not applicable.

Competing interests
The authors declare that they have no known competing financial interests or personal relationships that could have appeared to influence the work reported in this paper.

Author details
[1]Suzhou Institute of Biomedical Engineering and Technology, Chinese Academy of Sciences, Suzhou, Jiangsu, China
[2]School of Biomedical Engineering (Suzhou), Division of Life Sciences and Medicine, University of Science and Technology of China, Hefei, Anhui, China
[3]Xuzhou Medical University, Xuzhou, Jiangsu, China
[4]Department of Vascular Surgery, The Second Affiliated Hospital of Soochow University, Suzhou, Jiangsu, China

Received: 13 November 2024 / Accepted: 29 January 2025
Published online: 21 February 2025

References

1. Sun H, Saeedi P, Karuranga S, Pinkepank M, Ogurtsova K, Duncan BB, Stein C, Basit A, Chan JCN, Mbanya JC, Pavkov ME, Ramachandaran A, Wild SH, James S, Herman WH, Zhang P, Bommer C, Kuo S, Boyko EJ, Magliano DJ. IDF Diabetes Atlas: Global, regional and country-level diabetes prevalence estimates for 2021 and projections for 2045. Diabetes Res Clin Pract. 2022;183:109119.
2. McDermott K, Fang M, Boulton AJM, Selvin E, Hicks CW. Etiology, epidemiology, and disparities in the Burden of Diabetic Foot Ulcers. Diabetes Care. 2023;46:209–21.
3. Patel S, Srivastava S, Singh MR, Singh D. Mechanistic insight into diabetic wounds: Pathogenesis, molecular targets and treatment strategies to pace wound healing. Biome Pharmacother. 2019;112.
4. Li S, Nih LR, Bachman H, Fei P, Li Y, Nam E, Dimatteo R, Carmichael ST, Barker TH, Segura T. Hydrogels with precisely controlled integrin activation dictate vascular patterning and permeability. Nat Mater. 2017;16:953–.
5. Briquez PS, Clegg LE, Martino MM, Gabhann FM, Hubbell JA. Design principles for therapeutic angiogenic materials. Nat Reviews Mater. 2016;1:15006.
6. Pak CS, Heo CY, Shin J, Moon SY, Cho SW, Kang HJ. Effects of a Catechol-Functionalized Hyaluronic Acid Patch combined with human adipose-derived stem cells in Diabetic Wound Healing. Int J Mol Sci. 2021;22.
7. Li W, Kandhare AD, Mukherjee AA, Bodhankar SL. Hesperidin, a plant flavonoid accelerated the cutaneous wound healing in streptozotocin-induced diabetic rats: role of TGF-ß/Smads and Ang-1/Tie-2 signaling pathways. EXCLI J. 2018;17:399–419.
8. Li Y, Zheng L, Xu X, Song L, Li Y, Li W, Zhang S, Zhang F, Jin H. Mesenchymal stem cells modified with angiopoietin-1 gene promote wound healing. Stem Cell Res Ther. 2013;4:113.
9. Wang N, Ji X, Wu Y, Zhou S, Peng H, Wang J, Yu S, Zhang J. The different Molecular Code in Generation of dopaminergic neurons from astrocytes and mesenchymal stem cells. Int J Mol Sci. 2021;22.
10. An L, Tao Q, Wu Y, Wang N, Liu Y, Wang F, Zhang L, Shi A, Zhou X, Yu S, Zhang J. Synthesis of SPIO Nanoparticles and the Subsequent Applications in Stem Cell Labeling for Parkinson's Disease. Nanoscale Res Lett. 2021;16.
11. Baudin B, Bruneel A, Bosselut N, Vaubourdolle M. A protocol for isolation and culture of human umbilical vein endothelial cells. Nat Protoc. 2007;2:481–5.
12. Peng H, Du F, Wang J, Wu Y, Wei Q, Chen A, Duan Y, Shi S, Zhang J, Yu S. Adipose-Derived Stem-Cell-Membrane-Coated PLGA-PEI Nanoparticles Promote Wound Healing via Efficient Delivery of miR-21. Pharmaceutics. 2024;16.
13. Ren JS, Bai W, Ding JJ, Ge HM, Wang SY, Chen X, Jiang Q. Hypoxia-induced AFAP1L1 regulates pathological neovascularization via the YAP-DLL4-NOTCH axis. J Transl Med. 2023;21:651.
14. Lu Y, Han G, Zhang Y, Zhang L, Li Z, Wang Q, Chen Z, Wang X, Wu J. M2 macrophage-secreted exosomes promote metastasis and increase vascular permeability in hepatocellular carcinoma. Cell Communication Signal. 2023;21:299.
15. Du F, Liu M, Wang J, Hu L, Zeng D, Zhou S, Zhang L, Wang M, Xu X, Li C, Zhang J, Yu S. Metformin coordinates with mesenchymal cells to promote VEGF-mediated angiogenesis in diabetic wound healing through Akt/mTOR activation. Metabolism. 2023;140:155398.
16. Yu W, Zhou H, Feng X, Liang X, Wei D, Xia T, Yang B, Yan L, Zhao X, Liu H. Mesenchymal stem cell secretome-loaded fibrin glue improves the healing of intestinal anastomosis. Front Bioeng Biotechnol. 2023;11:1103709.
17. Mehanna RA, Nabil I, Attia N, Bary AA, Razek KA, Ahmed TA, Elsayed F. The effect of bone marrow-derived mesenchymal stem cells and their conditioned media topically delivered in Fibrin glue on Chronic Wound Healing in rats. Biomed Res Int. 2015;2015:846062.
18. Niu Q, He J, Wu M, Liu J, Lu X, Zhang L, Jin Z. Transplantation of bone marrow mesenchymal stem cells and fibrin glue into extraction socket in Maxilla promoted bone regeneration in osteoporosis rat. Life Sci. 2022;290:119480.
19. Saharinen P, Eklund L, Alitalo K. Therapeutic targeting of the angiopoietin–TIE pathway. Nat Rev Drug Discovery. 2017;16:635–61.
20. Tiruppathi C, Wang D-M, Ansari MO, Bano S, Tsukasaki Y, Mukhopadhyay A, Joshi JC, Loch C, Niessen HWM, Malik AB. Ubiquitin ligase CHFR mediated degradation of VE-cadherin through ubiquitylation disrupts endothelial adherens junctions. Nat Commun. 2023;14.
21. Lagendijk AK, Hogan BM. VE-cadherin in vascular development: a coordinator of cell signaling and tissue morphogenesis. Curr Top Dev Biol. 2015;112:325–52.
22. Saxton RA, Sabatini DM. mTOR Signaling in Growth, Metabolism, and Disease. Cell. 2017;168:960–76.
23. Wang J, Cui B, Chen Z, Ding X. The regulation of skin homeostasis, repair and the pathogenesis of skin diseases by spatiotemporal activation of epidermal mTOR signaling. Front cell Dev Biology. 2022;10.
24. Yao W, Wang Z, Ma H, Lin Y, Liu X, Li P, He X. Epithelial-mesenchymal plasticity (EMP) in wound healing: exploring EMT mechanisms, regulatory network, and therapeutic opportunities. Heliyon. 2024;10.
25. Yano K, Brown LF, Detmar M. Control of hair growth and follicle size by VEGF-mediated angiogenesis. J Clin Invest. 2001;107:409–17.
26. Peña OA, Martin P. Cellular and molecular mechanisms of skin wound healing. Nat Rev Mol Cell Bio. 2024;25:599–616.
27. Luo Z, Tian M, Yang G, Tan Q, Chen Y, Li G, Zhang Q, Li Y, Wan P, Wu J. Hypoxia signaling in human health and diseases: implications and prospects for therapeutics. Signal Transduct Target Therapy. 2022;7:218.
28. Tsao CC, Baumann J, Huang SF, Kindler D, Schroeter A, Kachappilly N, Gassmann M, Rudin M, Ogunshola OO. Pericyte hypoxia-inducible factor-1 (HIF-1) drives blood-brain barrier disruption and impacts acute ischemic stroke outcome. Angiogenesis. 2021;24:823–42.
29. Wietecha MS, Król MJ, Michalczyk ER, Chen L, Gettins PG, DiPietro LA. Pigment epithelium-derived factor as a multifunctional regulator of wound healing. Am J Physiol Heart Circ Physiol. 2015;309:H812–26.
30. DiPietro LA. Angiogenesis and wound repair: when enough is enough. J Leukoc Biol. 2016;100:979–84.
31. Tattersall IW, Du J, Cong Z, Cho BS, Klein AM, Dieck CL, Chaudhri RA, Cuervo H, Herts JH, Kitajewski J. In vitro modeling of endothelial interaction with macrophages and pericytes demonstrates notch signaling function in the vascular microenvironment. Angiogenesis. 2016;19:201–15.
32. Thijssen VL, Paulis YW, Nowak-Sliwinska P, Deumelandt KL, Hosaka K, Soetekouw PM, Cimpean AM, Raica M, Pauwels P, van den Oord JJ, Tjan-Heijnen VC, Hendrix MJ, Heldin CH, Cao Y, Griffioen AW. Targeting PDGF-mediated recruitment of pericytes blocks vascular mimicry and tumor growth. J Pathol. 2018;246:447–58.
33. Hakanpaa L, Sipila T, Leppanen VM, Gautam P, Nurmi H, Jacquemet G, Eklund L, Ivaska J, Alitalo K, Saharinen P. Endothelial destabilization by angiopoietin-2 via integrin β1 activation. Nat Commun. 2015;6:5962.
34. Isidori AM, Venneri MA, Fiore D. Angiopoietin-1 and Angiopoietin-2 in metabolic disorders: therapeutic strategies to restore the highs and lows of angiogenesis in diabetes. J Endocrinol Invest. 2016;39:1235–46.
35. Kämpfer H, Pfeilschifter J, Frank S. Expressional regulation of angiopoietin-1 and– 2 and the tie-1 and– 2 receptor tyrosine kinases during cutaneous wound healing: a comparative study of normal and impaired repair. Lab Invest. 2001;81:361–73.
36. Balaji S, Han N, Moles C, Shaaban AF, Bollyky PL, Crombleholme TM, Keswani SG. Angiopoietin-1 improves endothelial progenitor cell-dependent neovascularization in diabetic wounds. Surgery. 2015;158:846–56.

37. Attia N, Mashal M, Puras G, Pedraz JL. Mesenchymal stem cells as a Gene Delivery Tool: promise, problems, and prospects. Pharmaceutics. 2021;13:843.
38. Zhang P, Dong J, Fan X, Yong J, Yang M, Liu Y, Zhang X, Lv L, Wen L, Qiao J, Tang F, Zhou Y. Characterization of mesenchymal stem cells in human fetal bone marrow by single-cell transcriptomic and functional analysis. Signal Transduct Target Therapy. 2023;8:126.
39. Cao M, Zhao Y, Chen T, Zhao Z, Zhang B, Yuan C, Wang X, Chen L, Wang N, Li C, Zhou X. Adipose mesenchymal stem cell-derived exosomal microRNAs ameliorate polycystic ovary syndrome by protecting against metabolic disturbances. Biomaterials. 2022;288:121739.
40. Zhang Y, Yan J, Liu Y, Chen Z, Li X, Tang L, Li J, Duan M, Zhang G. Human amniotic fluid stem cell-derived exosomes as a Novel cell-free therapy for cutaneous regeneration. Front cell Dev Biology. 2021;9:685873.
41. Mishra S, Sevak JK, Das A, Arimbasseri GA, Bhatnagar S, Gopinath SD. Umbilical cord tissue is a robust source for mesenchymal stem cells with enhanced myogenic differentiation potential compared to cord blood. Sci Rep. 2020;10:18978.
42. Han Y, Yang J, Fang J, Zhou Y, Candi E, Wang J, Hua D, Shao C, Shi Y. The secretion profile of mesenchymal stem cells and potential applications in treating human diseases. Signal Transduct Target Therapy. 2022;7:92.
43. Xiao Y, Li H, Zhang J, Yang S, Zhang C, Huang Y, Tang X, Xie H. Mesenchymal stem cell-derived exosomes: versatile nanomaterials for skin wound treatment. Nano Res. 2024;17:2836–56.
44. Karar J, Maity A. PI3K/AKT/mTOR pathway in Angiogenesis. Front Mol Neurosci. 2011;4:51.
45. He Y, Sun MM, Zhang GG, Yang J, Chen KS, Xu WW, Li B. Targeting PI3K/Akt signal transduction for cancer therapy. Signal Transduct Target Therapy. 2021;6:425.
46. Jere SW, Houreld NN, Abrahamse H. Role of the PI3K/AKT (mTOR and GSK3β) signalling pathway and photobiomodulation in diabetic wound healing. Cytokine Growth Factor Rev. 2019;50:52–9.
47. Schimmel L, Fukuhara D, Richards M, Jin Y, Essebier P, Frampton E, Hedlund M, Dejana E, Claesson-Welsh L, Gordon EJ. c-Src controls stability of sprouting blood vessels in the developing retina independently of cell-cell adhesion through focal adhesion assembly. Development. 2020;147.
48. Tang J, Kang Y, Zhou Y, Shang N, Li X, Wang H, Lan J, Wang S, Wu L, Peng Y. TIMP2 ameliorates blood-brain barrier disruption in traumatic brain injury by inhibiting src-dependent VE-cadherin internalization. J Clin Invest. 2023;134.
49. Azzi S, Hebda JK, Gavard J. Vascular permeability and drug delivery in cancers. Front Oncol. 2013;3:211.
50. Gao F, Sabbineni H, Artham S, Somanath PR. Modulation of long-term endothelial-barrier integrity is conditional to the cross-talk between Akt and Src signaling. J Cell Physiol. 2017;232:2599–609.
51. Kamal R, Awasthi A, Pundir M, Thakur S. Healing the diabetic wound: unlocking the secrets of genes and pathways. Eur J Pharmacol. 2024;975:176645.
52. Bonnici L, Suleiman S, Schembri-Wismayer P, Cassar A. Targeting signalling pathways in Chronic Wound Healing. Int J Mol Sci. 2023;25.
53. Zhou S, Li Z, Li X, Ye Y, Wang M, Jiang J, Tao L, Wang Y, Tung C-T, Chung Y, Kim E, Shen X, Xu X, Xiang X, Xie Q, Zhang J, Wu W, Lin X, Chuong C-M, Lei M. Crosstalk between endothelial cells and dermal papilla entails hair regeneration and angiogenesis during aging. J Adv Res. 2024. https://doi.org/10.1016/j.jare.2024.05.006
54. Wallace RG, Rochfort KD, Barabas P, Curtis TM, Uehara H, Ambati BK, Cummins PM. COMP-Ang1: therapeutic potential of an engineered Angiopoietin-1 variant. Vascul Pharmacol. 2021;141:106919.

Publisher's note

Springer Nature remains neutral with regard to jurisdictional claims in published maps and institutional affiliations.